CONF-970233--3

SAN096-2576C
SAND--96-2576C

STRUCTURAL DYNAMICS MODELING AND TESTING OF THE DEPARTMENT OF ENERGY TRACTOR/TRAILER COMBINATION

Richard V. Field, Jr.†, John E. Hurtado‡, Thomas G. Carne‡, and Clark R. Dohrmann†

† *Structural Dynamics and Vibration Control*
Sandia National Laboratories
P.O. Box 5800
Albuquerque, New Mexico 87185-0439

‡ *Experimental Structural Dynamics*
Sandia National Laboratories
P.O. Box 5800
Albuquerque, New Mexico 87185-0557

ABSTRACT. *This study presents a combined analytical and experimental effort to characterize and improve the ride quality of the Department Of Energy tractor/trailer combination. The focus is to augment the experimental test results with the use of a high quality computer model. The discussion includes an overview of the finite element model of the vehicle and experimental modal test results. System identification techniques are employed to update the mathematical model. The validated model is then used to illustrate the benefits of incorporating two major design changes, namely the switch from a separate cab/sleeper configuration to an integrated cab, and the use of a cab suspension system.*

NOMENCLATURE

c	Damping
g	Unit of acceleration
k	Stiffness
rms	Root-mean-square
$L(f)$	Insertion Loss Factor
$S(f)$	Power Spectral Density (PSD) Function
FRF	Frequency Response Function
MAC	Modal Assurance Criterion
MIF	Modal Indicator Function
RSI	Ride Severity Index

1. INTRODUCTION

Designing trucks that exhibit good ride characteristics has been a challenge to automotive engineers for many years. When attempting to improve ride quality, the response of primary interest is the vibration experienced by the driver and bunk occupants. The ride environment of the truck driver is influenced by road roughness, rotating tire/wheel assemblies, the driveline, and the engine [6]. In this study, only the ride due to external road surface excitation is considered.

Previous methods to improve cab-ride quality included altering the frame bending stiffness, introducing softer primary suspensions, and improving tire stability and driver seats [3]. The idea of a cab suspension system was first employed in heavy truck design more than three decades ago and consisted of an independent leaf spring assembly placed at each of the four corners of the cab [4]. Since then, the design of the cab suspension system has evolved into a fixed-front pivot combined with a spring/damper rear mount, and is very common on the road today.

2. FINITE ELEMENT MODEL

Figure 1 illustrates the MSC/NASTRAN finite element model of the DOE tractor/trailer combination. Currently, the cab, sleeper, and trailer are modeled as rigid body elements; each has a concentrated mass element associated with it located at the center-of-mass, and appropriate rigid element connections join these point masses to the remainder of the vehicle. One particular interface is located at the fifth wheel, where the tractor and trailer connect. The fifth wheel itself is modeled as a point mass, including the effects of the steel mounting plate that adds significant stiffness to the tractor frame. At the top of the fifth wheel is the king pin, which allows relative rotation in the X and Y directions between the tractor and trailer. Another interface occurs where linear springs model the cab and sleeper "hard-mounts" to the truck frame. These mounts exhibit stiffness in the three translational directions, and are situated in a 3-point and 4-point configuration, respectively. The tractor frame and crossmembers are modeled with a large number of QUAD elements that capture the frame elastic modes.

A detailed view of the steer axle suspension system is illustrated in Fig. 2, where the leaf spring is modeled as a simple linear spring in the vertical direction, and "very stiff" in the

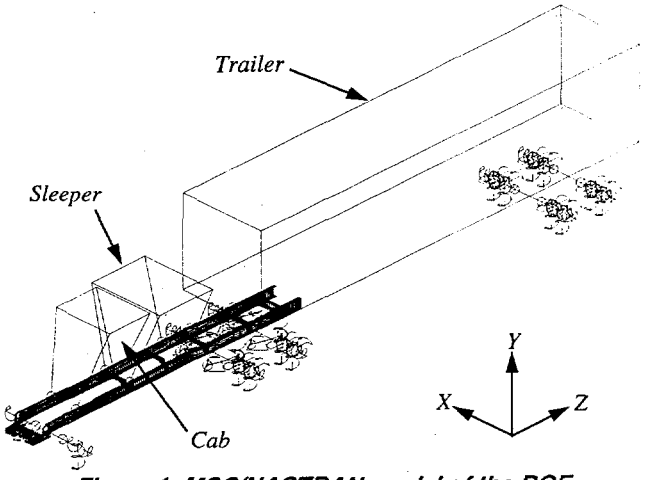

Figure 1: MSC/NASTRAN model of the DOE tractor/trailer combination.

This work was supported by the United States Department of Energy under Contract DE-AC04-94AL 85000.
Sandia is a multiprogram laboratory operated by Sandia Corporation, a Lockheed Martin Company, for the United States Department of Energy.

DISCLAIMER

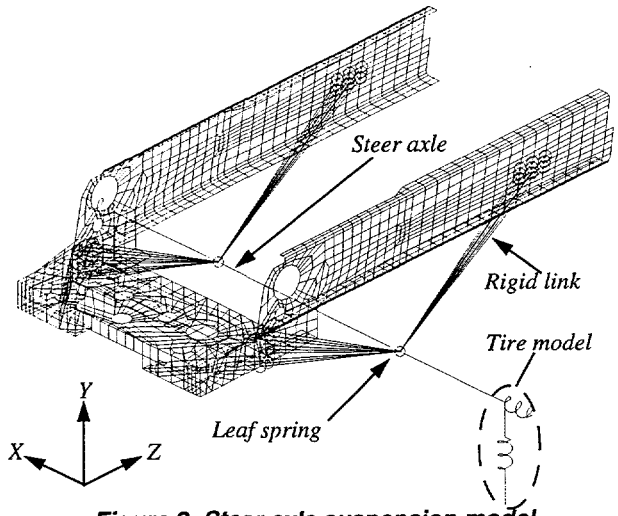

Figure 2: Steer axle suspension model.

remaining five directions. The leaf spring is rigidly connected to both the steer axle and the truck frame. A linear tire model is used here, consisting of two spring elements that represent the effective stiffness in the vertical and lateral directions. Note that this is valid because only small displacements are expected in a modal test. There is no fore/aft stiffness for the tire because there are no brakes on the steer axle. Lastly, the axle model is a series of NASTRAN BEAM elements.

Figure 3 contains a detailed view of the Neway AD-246 suspension system used on both the front and rear tractor drive axles. Each suspension system utilizes a trailing arm, modeled as a rigid link, an airbag, modeled as a linear spring in the axial direction only, and anti-roll bar, modeled as a series of BEAM elements. The AD-246 also contains two shock absorbers (just in-board of the airbags) that connect the anti roll-bar to the frame cross-members. These were not modeled, however, since the experimental modal tests were

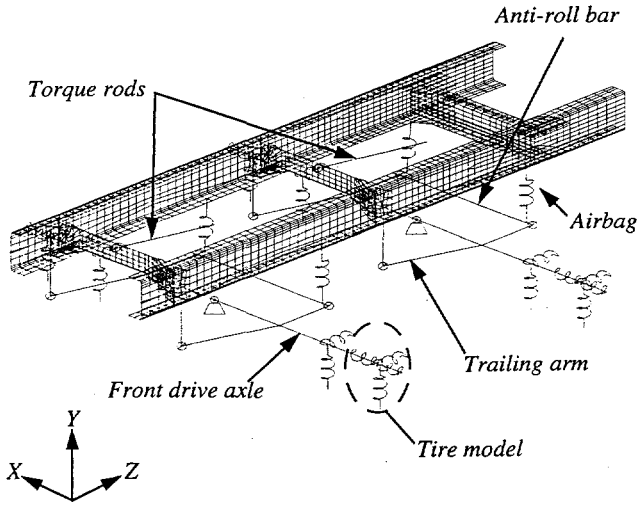

Figure 3: Drive axle suspension model.

performed with them disconnected. The tires (each axle contains four) are modeled identical to those on the steer axle, with one exception - an additional spring can be included to model the combined tire/brake stiffness in the fore/aft direction. This allows the NASTRAN model to simulate the vehicle modal response with and without the brakes applied. As before, the front and rear axles were modeled as a series of BEAM elements. The suspension systems on the trailer also utilize leaf springs, but with a much higher spring rate. Similarly, modal testing was performed with and without the brakes on the trailer, leading to a tire model identical to that on the tractor drive axles.

3. MODAL TESTING

Several modal tests were performed on the vehicle. Tests were applied with and without the brakes applied, but only the latter case is discussed herein. Electrodynamic shakers rated at 50 lb, 100 lb, and 250 lb were used to simultaneously excite the structure. The forces were applied in the vertical direction, while a total of 101 Endevco 7751 accelerometers monitored the vibrational response of the system.

A low level, continuous-random force excitation signal was input to the vehicle through the electrodynamic shakers at two locations on the vehicle; the 100 lb shaker was located at the front/passenger side of the tractor, and the larger shaker was placed at the passenger side of the trailer, halfway back. The signals sufficiently excited the structure while keeping the dynamic response within the linear regime about the static equilibrium. Frequency response functions (FRFs) between the applied excitation forces and the measured accelerations were calculated and recorded. Modal frequencies, damping factors, and mode shapes were then estimated from the recorded FRFs.

The modal survey of the vehicle without the brakes applied was performed by releasing the applied brakes and rolling the vehicle forward to overcome any stiction in the wheels and bearings. Figure 4 shows experimental FRFs for this test

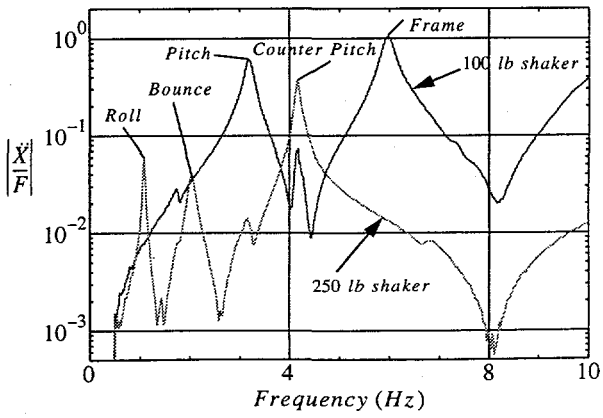

Figure 4: Experimental FRF.

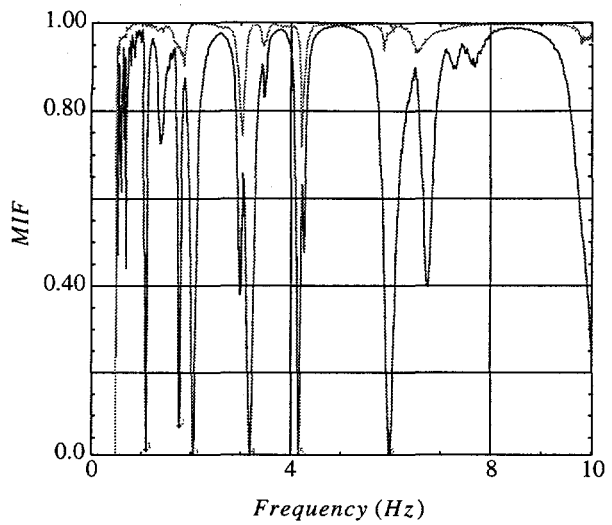

Figure 5: Experimental MIF.

configuration, and Fig. 5 shows the Mode Indicator Functions (MIFs). Table 2 lists the estimated natural frequencies from the data analysis, along with a brief description of the mode shapes. Both the experimental and analytical mode shapes are displayed in Figs. 6 through 11.

4. TEST/ANALYSIS CORRELATION

In order to obtain good agreement between the finite element model and modal test results, it was necessary to change the values of some uncertain parameters in the model. Six of the parameters that were updated are shown in Table 1. The original parameter values lead to large errors in the frequencies of the model. In addition, the mode shapes did not correlate well, as indicated by poor initial MAC values. These rather large discrepancies can be attributed to a lack of sufficient information to initially estimate the stiffnesses of the various suspensions and tire/wheel assemblies.

Parameter	Original	Updated
Tire vertical stiffness	4568, $\frac{lb}{in}$	11750, $\frac{lb}{in}$
Tire lateral stiffness	1500, $\frac{lb}{in}$	2080, $\frac{lb}{in}$
Tire fore/aft stiffness	2015, $\frac{lb}{in}$	2580, $\frac{lb}{in}$
Tractor leaf spring stiffness	2050, $\frac{lb}{in}$	8340, $\frac{lb}{in}$
Air bag stiffness	2100, $\frac{lb}{in}$	1040, $\frac{lb}{in}$
Trailer leaf spring stiffness	14000, $\frac{lb}{in}$	16350, $\frac{lb}{in}$

Table 1: Parameter changes due to model update.

Updated parameter values were obtained using the in-house code PESTDY (Parameter Estimation for STructural DYnamics) and lead to the improved MAC and frequency agreement shown in Table 2 and Figs. 6-11.

Mode Description	Test/Analysis Frequency (Hz)	MAC
fore/aft	N/A / 0.211	N/A
roll/twist #1	1.09 / 1.08	0.980
roll/twist #2	1.76 / 1.76	N/A
bounce	2.04 / 2.01	0.867
pitch	3.19 / 3.22	0.939
counter pitch	4.16 / 4.12	0.835
bending	5.96 / 6.06	0.830

Table 2: Results of model update.

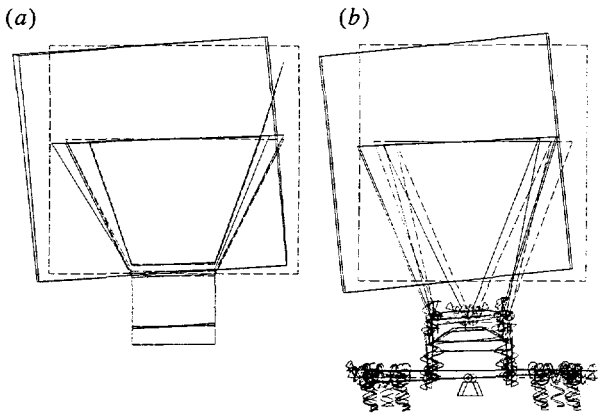

Figure 6: Roll/twist mode #1, experimental, (a), and analytical, (b).

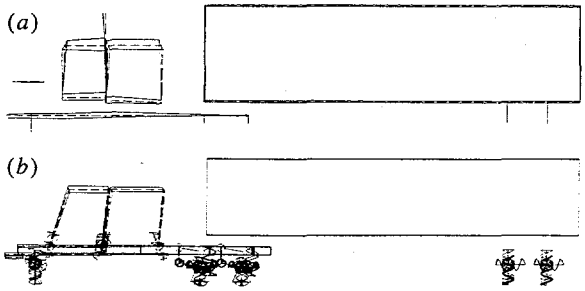

Figure 7: Roll/twist mode #2, experimental, (a), and analytical, (b).

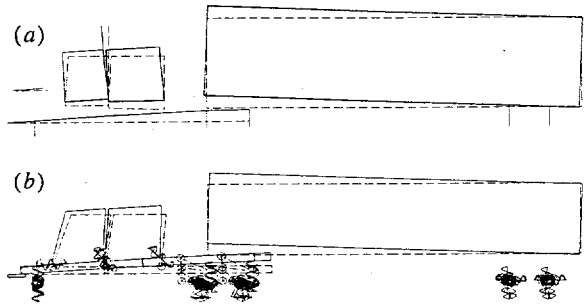

Figure 8: Bounce mode, experimental, (a), and analytical, (b).

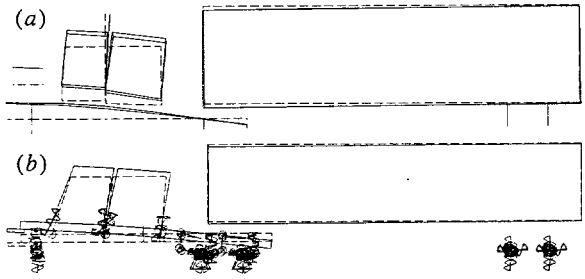

Figure 9: Pitch mode, experimental, (a), and analytical, (b).

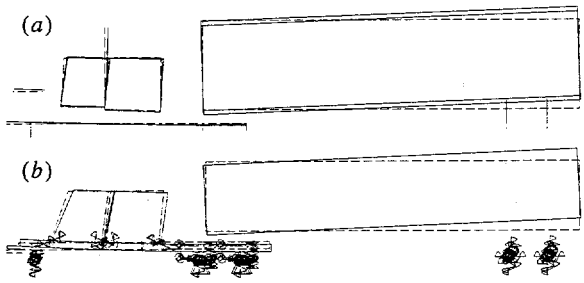

Figure 10: Counter pitch mode, experimental, (a), and analytical, (b).

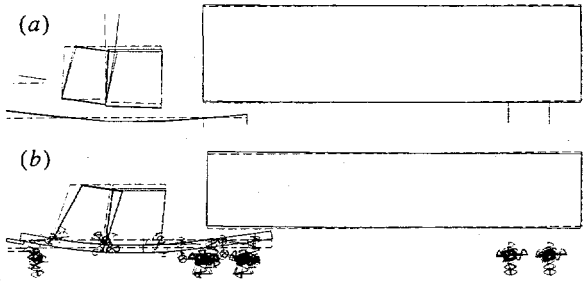

Figure 11: Frame bending mode, experimental, (a), and analytical, (b).

A few comments concerning the results of the test/analysis correlation are in order. Because the correlation was performed using modal test data, the updated parameters are associated with small amplitude motions. It is expected that some stiffnesses, such as those of the leaf springs, would be reduced in over-the-road environments where stiction effects are overcome. Efforts are currently underway to obtain stiffness and damping estimates directly from the transient response of driving the vehicle over a prescribed bump. Finally, it is noted that there remains some uncertainty in the absolute values of the tire vertical and suspension stiffnesses because they act in series.

5. DESIGN WORK

The design of a next-generation DOE tractor is to be completed in the next few years. This new vehicle will most likely exhibit significant modifications from the current design. One such change may be a switch to an integrated cab configuration, since this provides more room to the occupants. Another might be the addition of a tractor cab suspension system to improve the vibrational response of the cab. In this paper, the authors examine the performance of a cab suspension system that is available on the market today. In addition, an optimized suspension will also be considered. This cab suspension system is optimal in the sense that it provides the maximum protection to the driver from vibration due to road surface input.

For the purposes of this study, the suspension is modeled as a simple spring-damper system and is placed into the full updated finite element model with new integrated cab, as shown in Fig. 12. Furthermore, the stiffness and damping constants of this system are used as the design variables in the optimization problem to be discussed later. Linear springs in the three translational directions model the cab "hard-mounts" to the truck frame in the front.

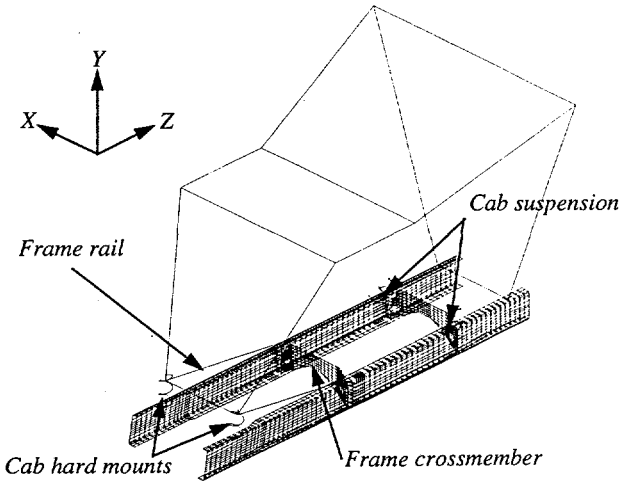

Figure 12: Integrated cab with cab suspension.

Frequency response and power spectral density analyses can be utilized to assess the vibratory response of automotive vehicles. Below are some results from such a study that simulates the DOE vehicle driving at 55 *m.p.h.* over a "rough road". Some theoretical concepts are presented, and analytical results using the model are discussed. Special emphasis is given to the issue of random loading and the cross-spectral density matrix that simulates the road input to an 18-wheel vehicle.

Most road surfaces have irregularities that are best described as random processes, and many can be accurately represented under an additional assumption of stationarity [5]. It is therefore relevant to study the vehicle response due to a stationary random "rough road" input at several key locations of the truck.

To apply this input PSD, knowledge of the cross-spectral density matrix of input forces is required. Assuming the vehicle is following a straight, constant speed trajectory, let W_1 and W_2 represent the amplitude seen by the left and right tires, respectively, due to the excitation of the road. For the studies presented here, it is assumed that the left and right tires experience the same road surface, but the two are not perfectly correlated. Define

$$\phi_{11}(\tau) = E[W_1(\tau)W_1(t+\tau)], \quad (1)$$

$$\phi_{22}(\tau) = E[W_2(\tau)W_2(t+\tau)], \quad (2)$$

$$\phi_{12}(\tau) = E[W_1(\tau)W_2(t+\tau)], \quad (3)$$

where $E[\bullet]$ is the expectation operator, $\phi_{11}(\tau)$ and $\phi_{22}(\tau)$ are the autocorrelation functions, and $\phi_{12}(\tau)$ is the crosscorrelation function representing the interaction between the left and right sides of the vehicle.

The schematic shown in Fig. 13. illustrates the 10 locations in which the "rough road" will excite the vehicle, assuming the dual wheel locations at stations 3 through 10 act together. The complete input power spectra is therefore characterized by a ten-by-ten matrix, where the elements of this matrix involve the Fourier transforms of Eqs. (1)-(3). Specifically, the two-by-two blocks on the diagonal of this matrix are of the form

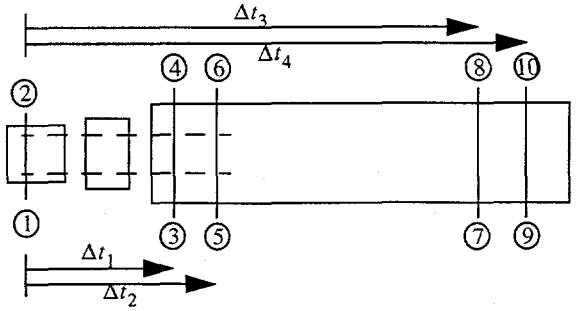

Figure 13: Input stations for the DOE tractor/trailer combination.

$$\Phi_{2x2}(f) = \begin{bmatrix} k_{eff}^2\phi_{11}(f) & k_{eff}^2\phi_{12}(f) \\ k_{eff}^2\phi_{12}(f) & k_{eff}^2\phi_{22}(f) \end{bmatrix}, \quad (4)$$

where k_{eff} is the effective stiffness at the particular station of interest (*i.e.*, the collective vertical tire stiffness), and $\phi_{11}(f)$, $\phi_{12}(f)$, and $\phi_{22}(f)$ are the Fourier transforms of Eqs. (1)-(3). Note that by scaling Eq. (4) by the stiffness terms, the input is now a *force* power spectral density.

The remaining terms of Φ involve various degrees of correlation between the different axles. Because the vehicle is at a constant speed, this can be accomplished by delaying the input to the tractor front drive axle, as well as those behind it [8], as illustrated in Fig. 13.

It has been found that terrain roughness can be represented in the frequency domain by power spectral density functions of the form

$$\Psi(\Omega) = c\Omega^{-n}, \quad (5)$$

where Ω is the spatial frequency, in units of *cycles/length*, and n and c are constants. As discussed in [5], $n = 2.0$ is typical. Therefore, for a vehicle traveling at a constant speed of v_o, the power spectral density that describes the input displacement seen at the road surface can be given by

$$\Phi(f) = \frac{1}{v_o}\Psi(\Omega) = \frac{v_o c}{(2\pi f)^2}, \quad (6)$$

where f is now the temporal frequency, in units of *cycles/sec.* In addition, plots of Ψ *vs.* Ω are presented in [1], [8] and [9] for several road surface types. Assuming a "rough road" terrain, $c = 3.24e\text{-}6$ *in-cycles.*

Figure 14 illustrates $\phi_{11}(f)$, $\phi_{22}(f)$, and $\phi_{12}(f)$ vs. frequency, where plot (a) is directly from Eq. (6) for $v_o = 55\ mph$. To estimate the correlation of the terrain between the left and right tire tracks of the vehicle, consider the coherency function

$$g^2(\Omega) = \frac{|\Psi_{12}(\Omega)|^2}{\Psi_{11}(\Omega)\Psi_{22}(\Omega)}, \quad 0 \le g^2(\Omega) \le 1 \quad (7)$$

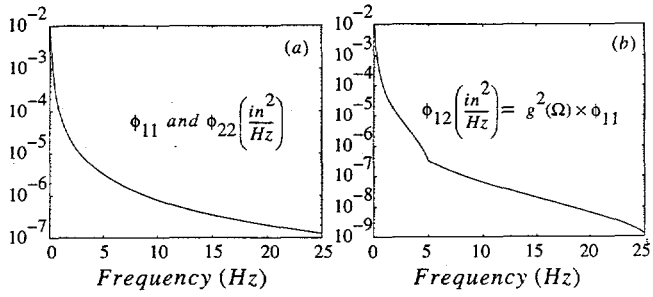

Figure 14: Input autopower and crosspower spectral density functions.

Typically, as discussed in [9], the coherency function is near unity at low frequencies (*i.e.*, high correlation for hills or dips in the road surface), and much lower at the higher frequencies (*i.e.*, low correlation for cracks in the pavement, potholes, etc.). Utilizing this assumption, Eq. (7) can be used to determine $\phi_{12}(f)$ shown in Fig. 14(b).

The cab suspension system, placed between the rear of the integrated cab and truck frame, can be utilized to improve the ride quality of the vehicle. The ride severity index (RSI), a weighted measure of the power of the output spectrum, can be used to gauge this improvement. Consider the following relation

$$RSI = \left[\int_{f_1}^{f_2} L(f)^2 S_{out}(f) df\right]^{\frac{1}{2}}, \tag{8}$$

where $S_{out}(f)$ is the output power spectral density function and $f \in [f_1, f_2]$ denotes the frequency band of interest. As shown, the RSI is a scalar quantity that is simply a weighted sum of the output PSD. The insertion loss factor, $L(f)$, is a quantity indicative of the human body's sensitivity to vibration. The higher the loss factor, the more sensitive the human is to the excitation.

For the studies included here, only the vibration at the driver seat is considered, and the ride severity index is given by

$$RSI = \left(\int_1^4 \frac{f}{4} S_Y(f) df + \int_4^8 S_Y(f) df + \int_8^{25} \left(\frac{64}{f^2}\right) S_Y(f) df + 1.96\left\{\int_1^2 S_Z(f) df + \int_2^{25} \left(\frac{4}{f^2}\right) S_Z(f) df\right\}\right)^{\frac{1}{2}} \tag{9}$$

The terms involving $S_Z(f)$ are scaled by an additional factor of $(1.4)^2 = 1.96$ since vibration in the fore/aft direction is particularly disturbing to humans [2].

The minimization problem to be solved here can be stated as

$$\min_{k,c,z} RSI, \text{ subject to } k_{min}, c_{min} \le k, c \le k_{max}, c_{max}, \tag{10}$$

where k, c, and z refer to the stiffness, damping, and location of the cab suspension system, respectively, and the bounds on the stiffness and damping ensure physically practical solutions. Because varying the location of the suspension system requires re-meshing the finite element model, however, Eq. (10) is solved for a fixed location, z. This location is then varied discreetly along the tractor frame to provide a qualitative estimate of the optimal location.

The optimization capabilities of MATLAB [7] are utilized to determine optimal values of the cab suspension system at various locations along the frame. The results are shown in Table 3, where z is the location of the suspension system, referenced to the location of truck's third frame crossmember (where a typical cab suspension would be located due to structural considerations). $z = 0$ is the typical location of the suspension, and positive and negative values of z are behind and in front of it, respectively. Note that the optimal spring-damper values are to be applied at both the passenger- and driver-side of the vehicle.

Design	k, $\frac{lb}{in}$	c, $\frac{lb\text{-}s}{in}$	RSI, $mg\text{-}rms$
Current cab	N/A	N/A	20.42
Current sleeper	N/A	N/A	23.53
z = 0.0 *in*	333.4	105.6	11.46
z = -12.0 *in*	420.0	125.1	11.07
z = -24.0 *in*	287.7	128.0	9.386
z = 12.0 *in*	410.5	101.6	11.44
z = 24.0 *in*	416.9	95.77	11.35

Table 3: RSI for current design (cols. 1 and 2) vs. integrated cab with optimal suspension.

Plots illustrating the possible benefits of an optimized cab suspension are included in Figs. 15 and 16, where it is evident that changing the design of the cab suspension only has a significant effect on the response of the cab in the frequency range of 0 to 6 *Hz*.

The optimal RSI occurs when the suspension is pushed 24 inches forward of its present location. The vertical response in Fig. 15 illustrate a drastic reduction in the bounce and pitch modes when using the optimal cab suspension. In addition, the vertical mode of the suspension reduces in frequency from $f = 1.34\ Hz$ to $f = 1.00\ Hz$ since, as the location of the cab suspension moves forward, it is required to carry

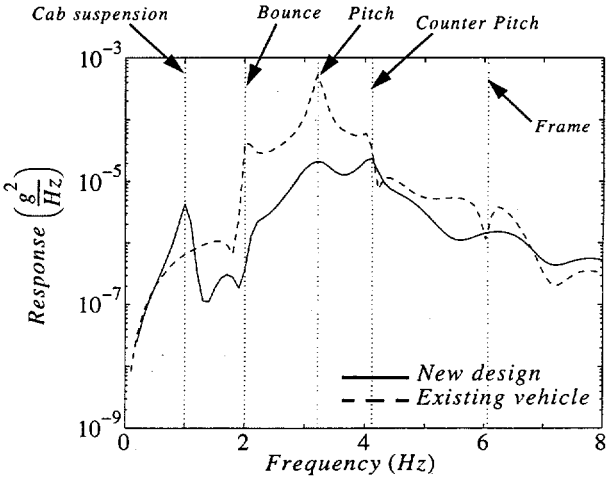

Figure 15: Vertical response at the cab of existing vehicle and new design.

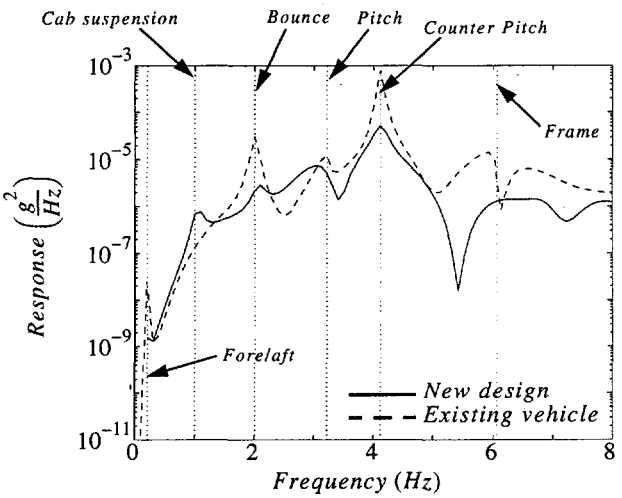

Figure 16: Fore/aft response at the cab of existing vehicle and new design.

more of the cab weight. When considering the fore/aft response of the cab, shown in Fig. 16, the optimal suspension again demonstrates reduction in the power of the bounce, pitch, and counter-pitch modes.

As a general observation, it appears that the RSI will continue to decrease as the location of the cab suspension is moved forward. There are physical limits, obviously, since moving the suspension forward requires that it support a greater static load due to weight of the cab. Cab stresses are also an issue and, therefore, the location of the cab suspension cannot be chosen to minimize the ride severity index alone.

6. CONCLUSIONS

The preliminary dynamic model of the DOE tractor/trailer combination correlates well with the characteristics seen during the experimental modal tests. As the model is refined, it is clear that it will be an integral tool in determining the design of the next-generation tractor. Any possible benefits to be gained from the use of available passive cab vibration suppression methods will be researched. In addition, the computer model can be used to examine any improvements utilizing active vibration control techniques.

Possible design modifications to the vehicle, namely the conversion to an integrated-type cab with a cab suspension system, have been discussed. With the addition of the integrated cab with nominal cab suspension, a 44% reduction in ride severity can be achieved over the current cab/sleeper configuration, which is hard-mounted to the truck frame. Furthermore, once an optimized cab suspension is utilized, the RSI can be reduced by an additional 18%. Finally, the results shown here indicate that the cab suspension system should be located as far forward as structural considerations will allow.

7. ACKNOWLEDGEMENTS

The authors would like to acknowledge the help of Rob Pirtle and Hoden Farrah of Marmon Motors and Ken Vande Brake of Link Manufacturing, Inc.

8. REFERENCES

[1] Baum, J.M., J.A. Bennett and T.G. Carne, "Truck Ride Improvement Using Analytical and Optimization Methods," General Motors Research Laboratories, GMR-2324-R, 1978.

[2] "Evaluation of Human Exposure to Whole-Body Vibration," International Organization for Standardization, ISO 2631/1-1985(E).

[3] Flower, W., "Analytical and Subjective Ride Quality Comparison of Front and Rear Cab Isolation Systems on a COE Tractor," *Society of Automotive Engineers*, No. 780411, pp. 1917-1929, 1978.

[4] Foster, A.W., "A Heavy Truck Cab Suspension for Improved Ride," *Society of Automotive Engineers*, No. 780408, pp. 1899-1916, 1978.

[5] Gillespie, T.D., *Fundamentals of Vehicle Dynamics*, Society of Automotive Engineers, 1992.

[6] Gillespie, T.D., "Heavy Truck Ride, Society of Automotive Engineers, The Thirty-First L. Ray Buckendale Lecture, SP-607, 1985.

[7] Grace, A., "MATLAB Optimization Toolbox," The MathWorks, 1995.

[8] Healy, A.J., "An Analytical and Experimental Study of Automobile Dynamics with Random Roadway Inputs," *ASME Journal of Dynamic Systems, Measurement, and Control*, December, pp. 284-292, 1977.

[9] Soong, T.T. and M. Grigoriu, *Random Vibration of Mechanical and Structural Systems*, Prentice-Hall, Inc., 1993.